Inviscid Shear Flow Analysis of Corner Eddies Ahead of a Channel Flow Contraction

R. N. Meroney
Professor,
Fluid Mechanics and
Wind Engineering Program,
Department of Civil Engineering,
Colorado State University,
Fort Collins, CO 80523

The steady rotational flow of an inviscid fluid in a two-dimensional channel toward a sink or a contraction is treated. The velocity distribution at upstream infinity is approximated by a linear combination of uniform flow, linear shear flow, and a cosine curve. The combinations were adjusted to simulate flows ranging from laminar to turbulent. Vorticity is assumed conserved on streamlines. The resulting linear equations of motion are solved exactly. The solution show the dependence of the corner eddy separation and reattachment on flow geometry and approach flow vorticity and velocity distribution typified by a shape factor.

Introduction

When a viscous fluid flows in a channel or pipe toward an abrupt contraction eddies form in the corners immediately preceding that contraction. The shape of the corner eddies and their upwind extent are said to be functions of the upwind profile, viscosity, and the state of the fluid (laminar or turbulent). Yet, surprisingly, viscosity is not required to reproduce the phenomenon of separation and reattachment! This paper will examine a variety of inviscid flow configurations during which corner eddies appear in a two dimensional channel flow contraction and relate the size of the eddy to different descriptors of the approach flow.

Because of the complex nature of separation dynamics realistic theoretical models including exact solutions for the separation flow are limited. There is an extensive literature on well separated flows about bluff bodies and subsequent wake development (Wu, 1972; Thwaites, 1960). To produce realistic flow patterns most analyses depend upon measurements to specify undefined base pressure, prespecification of separation or reattachment points, and almost all are limited to uniform or linear velocity gradient approach flows (Kiya and Arie, 1972; Frenkiel, 1961). Numerical solutions for more general profiles of inviscid shear flow over boundary obstructions have been performed by some authors (Taulbee and Robertson, 1972; Bouwmeester, Meroney, and Sandborn, 1978), but they are not exact and can suffer from numerical empericism.

An interesting exception is the solution obtained by Yih (1959) for the inviscid shear flow of a cosine velocity profile in a two dimensional channel flowing into a corner sink. The key to an exact solution of the inviscid shear flow problem is to find a flow where the vorticity is a unique function of the streamline along which it is convected (Taulbee and Robertson, 1972). In such a situation no singular surfaces occur in the flow, but the solution are unlikely to represent exactly the corresponding flow of a real fluid even at large Reynolds number. (As noted by Yih (1959) this is part of the penalty for ignoring viscous forces entirely in the search for an exact analytic solution.) Nonetheless the flow exterior to the corner eddy is strikingly similar to those in front of actual separation bubbles (Pande, Prakash, and Argarwal, 1980; Good and Joubert, 1968; Robertson and Taulbee, 1969; or Bradshaw and Galea, 1967), and the similarity justifies further examination of such exact solutions.

Two-Dimensional Channel Flow Into a Line Sink

In this section we shall consider steady two-dimensional flow in a long channel with half-width equal to unity terminating in a wall with a symmetrically placed line sink, with the centerline of the channel as the x-axis extending in the negative x direction.

Let ψ be Lagrange's stream function, then the equation governing steady two-dimensional inviscid flow is the Poisson equation or

$$\nabla^2\psi = \frac{\partial^2\psi}{\partial x^2} + \frac{\partial^2\psi}{\partial y^2} = -f(\psi) \tag{1}$$

where $-f(\psi)$ represents the vorticity and depends on the stream function alone. Ideally the velocity far upstream would be parabolic or logarithmic to represent the movement of a laminar or turbulent flow respectively in a long channel. Unfortunately the use of such profiles would make equation (1) nonlinear and preclude a simple solution. Instead we shall use a linear combination of uniform flow, a linear shear gradient, and a cosine distribution to create various nonuniform profiles. In terms of the centerline velocity U_{max} the dimensionless upstream profile is then

$$U/U_{max} = u_0 + K_0(1-y) + (1-u_0-K_0/2)\cos(\pi y/2) \tag{2}$$

which vanishes at the walls ($y = \pm 1$) and is maximum at the centerline. The corresponding dimensionless stream function far upstream is

Contributed by the Fluids Engineering Division for publication in the JOURNAL OF FLUIDS ENGINEERING. Manuscript received by the Fluids Engineering Division, September 27, 1983.

CEP83-84RNM-6

larger than the mean value during the entire duration of the adverse pressure gradient which suggests that the adverse part of the pressure gradient enhances the rate of production of turbulent kinetic energy. A non-sinusoidal pulsation may in fact increase the mean production rate and we plan to investigate this in the future.

6 Conclusions

Our numerical simulation of pulsed turbulent pipe flow indicates a negligible change in momentum transport despite the fact that a large pulsation amplitude was used and the frequency was in the frozen viscosity regime. This result would appear to cast doubt on Lemlich's [3] speculation that heat transfer rates can be significantly enhanced by pulsing at high frequencies. On the other hand, we found that the ensemble averaged fluctuation intensities and turbulence production rate showed strong phase dependence. One of the more striking results was that the production rate was largest during the part of the pulsation cycle when an adverse pressure gradient existed.

Acknowledgments

This work was supported by the Department of Energy under contract DE-AC02-82ER12033.A000. The calculations were performed on the IBM 4341 computer at Clarkson University.

References

1 Mizushina, T., Maruyama, T., and Shiozaki, Y., "Pulsating Turbulent Flow in a Tube," *J. Chem. Eng. Japan*, Vol. 6, Dec. 1973, pp. 487–494.

2 Mizushina, T., Maruyama, T., and Hirasawa, H., "Structure of the Turbulence in Pulsating Pipe Flows," *J. Chem. Eng. Japan*, Vol. 8, June 1975, pp. 210–216.

3 Lemlich, R., "Vibration and Pulsation Boost Heat Transfer," *Chem. Eng.*, Vol. 68, May 1961, pp. 171–176.

4 McLaughlin, J. B., Reddy, V., and Nunge, R. J., "A Model of the Viscous Wall Region of Turbulent Shear Flows," (submitted to *Chemical Engineering Communications*).

5 Reddy, V., "A Study of Steady and Pulsed Turbulent Pipe Flow," Ph.D. thesis, Clarkson College, Jan. 1984.

6 Hogenes, J. H. A., and Hanratty, T. J., "The Use of Multiple Wall Probes to Identify Coherent Patterns in the Viscous Wall Region," *J. Fluid Mech.*, Vol. 124, Nov. 1982, pp. 363–390.

7 Bakewell, H. P., and Lumley, J. L., "Viscous Sublayer and Adjacent Wall Region in Turbulent Pipe Flow," *Phys. Fluids*, Vol. 10, Sept. 1967, pp. 1880–1889.

8 Sirkar, K. K., "Turbulence in the Immediate Vicinity of a Wall and Fully Developed Mass Transfer at High Schmidt Numbers," Ph.D. thesis, U. of Illinois, 1969.

9 Brown, F. T., Margolis, D. L., and Shah, R. P., "Small Amplitude Frequency Behavior of Fluid Lines With Turbulent Flow," ASME *J. Basic Engineering*, Vol. 91, Dec. 1969, pp. 678–693.

10 Simpson, R. L., Shivaprasad, B. G., and Chew, Y.-T., "The Structure of a Separating Turbulent Boundary Layer. Part 4. Effects of Free-Stream Unsteadiness," *J. Fluid Mech.*, Vol. 127, Feb. 1983, pp. 219–261.

11 Morrison, W. R. B., Bullock, K. J., and Kronauer, R. E., "Experimental Evidence of Waves in the Sublayer," *J. Fluid Mech.*, Vol. 47, June 1971, pp. 639–656.

12 Orszag, S. A., and Kells, L. C., "Turbulence in Plane Poisuelle and Plane Couette Flow," *J. Fluid Mech.*, Vol. 96, Jan. 1980, pp. 159–205.

13 Lamb, H., *Hydrodynamics*, 6th edition, Dover Publications, New York, 1945.

14 Tu, S. W., and Ramaprian, B. R., "Fully Developed Periodic Turbulent Pipe Flow. Part 1. Main Experimental Results and Comparison with Predictions," *J. Fluid Mech.*, Vol. 137, Dec. 1983, pp. 31–58.

15 Tu, S. W., and Ramaprian, B. R., "Fully Developed Periodic Turbulent Pipe Flow. Part 2. The Detailed Structure of the Flow," *J. Fluid Mech.*, Vol. 137, Dec. 1983, pp. 59–81.

16 Shemer, L., and Kit, E., "An Experimental Investigation of the Quasisteady Turbulent Pulsating Flow in a Pipe," Phys. Fluids, Vol. 27, Jan. 1984, pp. 72–76.

17 Laufer, J., "The Structure of Turbulence in Fully Developed Pipe Flow," NACA Tech. Note 1174, 1954, pp. 417–434.

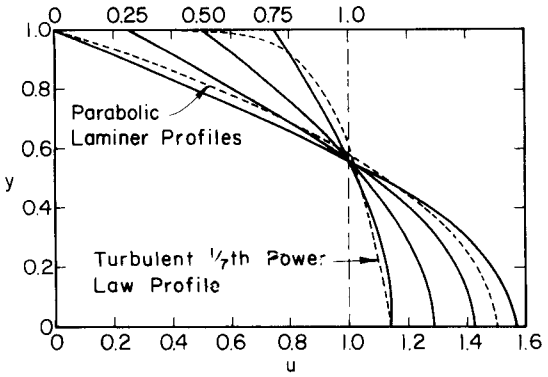

Fig. 1 Upstream velocity profiles, uniform plus cosine profiles

$$\psi = \int_0^y U/U_{max}\,dy$$

$$= u_0 y + K_0(y - y^2/2) + (1 - u_0 - K_0/2)\sin(\pi y/2) \quad (3)$$

such that at the walls ($y = \pm 1$) the values are ± 1. The vorticity function is then linear and equal to

$$f(\psi) = -K_0 - (\pi/2)^2(1 - u_0 - K_0/2)\sin(\pi y/2) \quad (4)$$

Note that for consistency $u_0 + K_0/2 < 1$ is required.

The boundary conditions on equation (1) are

(i) ψ = equation (3) as $x \to -\infty$. (5)

(ii) $\psi = \pm 1$ for $y = \pm 1$, and

(iii) $\psi = \pm 1$ for $y \lesseqgtr 0$ and $x = 0$.

Solution of equations (1) to (5) by the method of separation of variables yields

$$\psi = u_0 y + K_0(y - y^2/2) + (1 - u_0 - K_0/2)\sin(\pi y/2) \quad (6)$$

$$+ \sum_{n=1}^{\infty} C1_n \sin(n\pi y)\exp(n\pi x)$$

$$+ \sum_{n=1}^{\infty} C2_n \sin(n\pi y)\exp((n^2 - 1/4)^{1/2}\pi x)$$

which satisfies boundary condition (i) and (ii), and the values of $C1_n$ and $C2_n$ are determined by Fourier expansion to satisfy boundary condition (iii) such that

$$C1_n = (2u_0 + K_0)/(n\pi) + 2K_0(\cos(n\pi) - 1)/(n\pi)^3 \quad (7)$$

and

$$C2_n = 2(1 - u_0 - K_0/2)(1 + \cos(n\pi)/(4n^2 - 1))/(n\pi).$$

Equations (6) and (7) are the solution. The series solution has been evaluated out to sufficient terms such that the stream function is known to five significant places for different values of u_0 and K_0. Figure 2(*a*) and 2(*b*) are typical derived flow patterns for the half channel.

The stream function is specified to vary between -1 to $+1$ across the channel, but the flow may be distributed in a variety of profiles. Figure 1 suggests a possible set of profiles resulting from combinations of uniform and cosine functions. Alternatively, uniform and ramp functions were used. The dashed lines are parabolic and 1/7th power law profiles typical of laminar and turbulent channel flow distributions. Each profile is characterized by the magnitude of the slip at the wall, u_0, and the wall vorticity, ω_0. In addition one can characterize the velocity distribution by a displacement thickness, δ^*, and a momentum thickness, θ, which may be combined into a shape factor ratio, $H = \theta/\delta^*$, where

$$\delta^* = \int_0^1 (U_{max} - U)dy/U_{max}, \text{ and} \quad (8)$$

$$\theta = \int_0^1 U(U_{max} - U)dy/U_{max}^2.$$

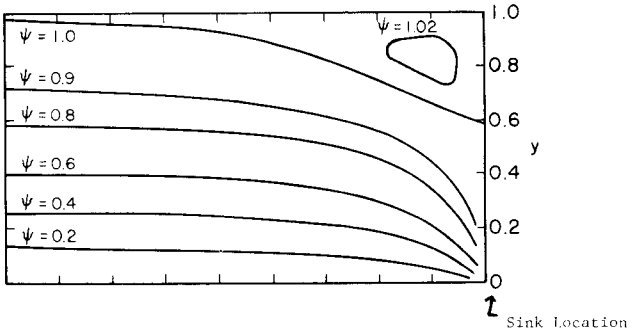

Fig. 2(*a*) Channel flow into a sink, $u_0 = 0.0$, $-u_0 = 2.47$

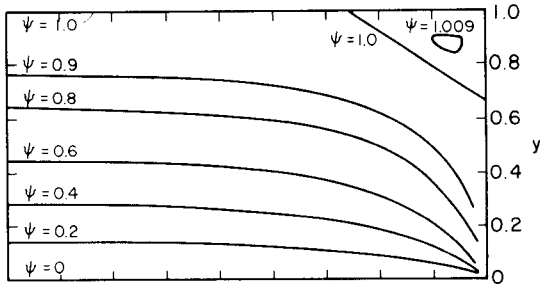

Fig. 2(*b*) Channel flow into a sink $u_0 = 0.25$, $-u_0 = 1.85$

Table 1 Influence of flow variables on separation and reattachment

u_0	K_0	$-\omega_0$	H	x_s	y_r
1.00	0	0	1.000	0	0
0	2.00	2.00	0.333	$-\infty$	0.40
0	0	2.47	0.376	$-\infty$	0.40
0.25	0	1.85	0.483	−0.51	0.33
0.50	0	1.24	0.619	−0.23	0.20
0.75	0	0.62	0.784	−0.06	0.04
0.25	1.50	1.50	0.425	−0.42	0.28
0.50	1.00	1.00	0.555	−0.18	0.13
0.75	0.50	0.50	0.735	−0.04	0.03
0.38	1.24	1.24	0.490	−0.32	0.20

Nomenclature

$C1_n$ = Fourier coefficient in infinite series
$C2_n$ = Fourier coefficient in infinite series
$f(\psi)$ = vorticity function
h = height of corner of contraction
h' = half width of contraction
H = shape factor
K_0 = gradient of linear shear profile
n = summation index in infinite series
U = velocity
U_{max} = velocity at $y = 0$
u_0 = slip velocity
x,y = Cartesian coordinates
x_s = distance of separation point from corner
y_r = distance to reattachment point from corner
ψ = stream function
δ^* = displacement thickness
θ = momentum thickness
ω_0 = vorticity at wall, $y = 1$

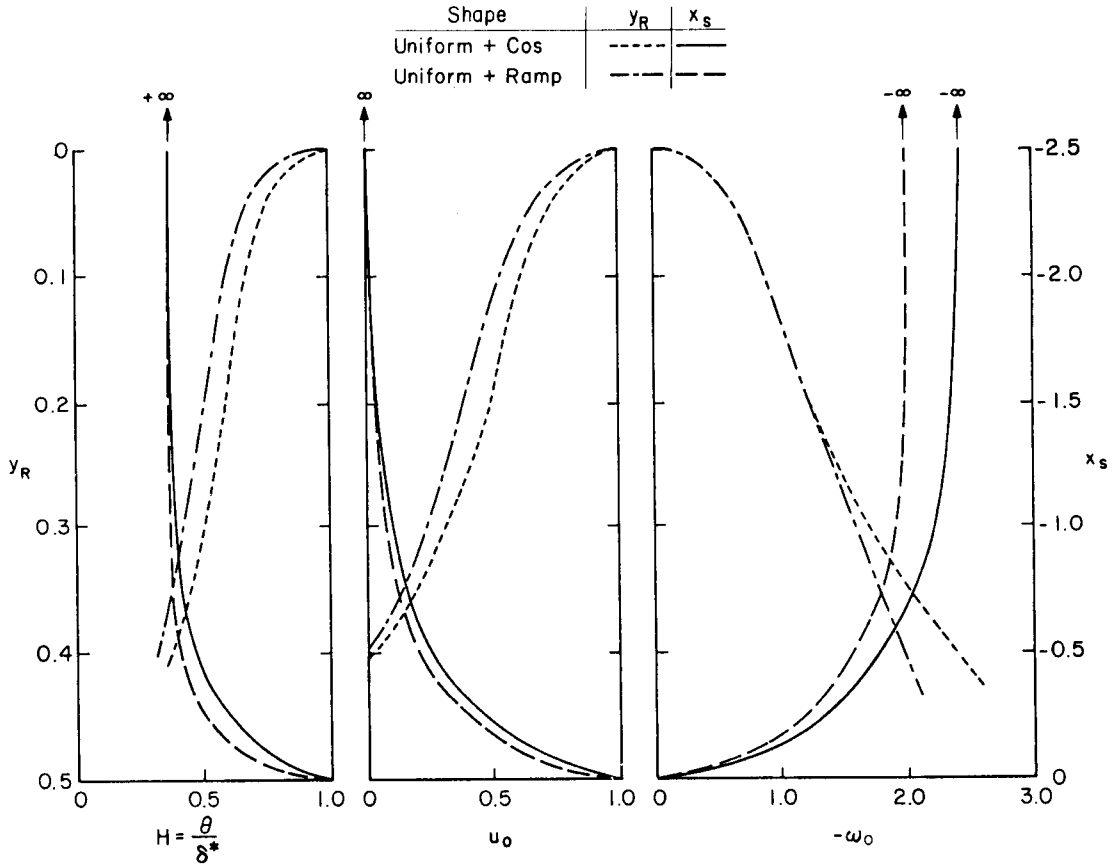

Fig. 3 Variation of separation distance and reattachment distance with profile parameters

Table 1 summarizes cases examined in this paper. Two flows are considered which maintain the same wall vorticity but different values of slip. Similarly one sees equal values of slip but different wall vorticity.

The size of the corner eddy is its most significant characteristic; hence, the distance to separation from the corner, x_s, and the location of the reattachment point, y_r, are also tabulated above. The variation of these variables with shape factor, slip velocity, and wall vorticity are plotted in Fig. 3.

As slip velocity approaches one, shape factor approaches one, or as vorticity decreases the corner eddy disappears. The rate of diminishing is not exactly the same for the various combinations of uniform, ramp and cosine flow, but they are very similar. As slip velocity decreases, shape factor decreases, and wall vorticity increases the reattachment point moves toward a value $y=0.6$ ($y_r=0.4$), but the separation point moves to $-\infty$. In the inviscid approach it appears a finite value of slip velocity is necessary to develop a finite separation point, x_s. Taulbee and Robertson (1972) also emphasized that the point of separation must be closely associated with the assumption about u_0. Indeed they conclude the entire inviscid flow field is sensitive to the choice of u_0.

Two-Dimensional Channel Flow Into a Contraction

In this section we will examine the effect of enlarging the hypothetical line sink into a finite width contraction. The new channel half width, h', may vary from 0.0 to 1.0. The channel contraction will confine the streamline pattern and result in larger exit velocities. When the contraction is abrupt the velocity profile will flatten and the flow will tend to separate at the corner. Since we will prespecify the exit profile the details of the post contraction eddy may not be realistic; nonetheless, the upstream corner eddy and flow field should be similar to measurements.

An exact solution can be obtained for two realistic exit profiles. The exit profile may be specified uniform such that $U_{x=0}/(U_{\max})_{x=-\infty}=1/h'$. Alternatively the exit profile can be a partial cosine shape with slip at the outer wall, i.e., $U_{x=0}/(U_{\max})_{x=-\infty}=\pi/2\ \cos(\pi y/2)/\sin(\pi h'/2)$. Neither of these profiles require that vertical velocities in the $x=0$ plane be zero (see Fig. 4).

Solutions for the contracted channel case can also be produced for an infinite combination of uniform, ramp, and cosine function upstream profiles. Since the sink solutions did not produce any unique perturbation resulting from the use of the ramp (linear shear flow) term the following solutions are limited to combinations of uniform and cosine profiles. As in the previous section the governing equations are (1) through (4), but with K_0 set to zero. The new boundary conditions for the uniform outlet flow case are

$$\begin{aligned} \text{(i)}\psi &= \text{equation (3) as } x\to-\infty \\ \text{(ii)}\psi &= \pm 1 \text{ for } y=\pm 1, \text{ and} \\ \text{(iii)}\psi &= y/h' \text{ for } -h'\le y\le h', \text{ or} \\ &= +1 \text{ for } h\le y\le 1, \text{ or} \\ &= -1 \text{ for } -1\le y\le -h'. \end{aligned} \tag{9}$$

The final solution for the stream function is then

$$\psi = u_0 y + (1-u_0)\sin(\pi y/2) + \sum_{n=1}^{\infty} C1_n \sin(n\pi y)\exp(n\pi x) + \sum_{n=1}^{\infty} C2_n \sin(n\pi y)\exp((n^2-\tfrac{1}{4})^{1/2}\pi x), \tag{10}$$

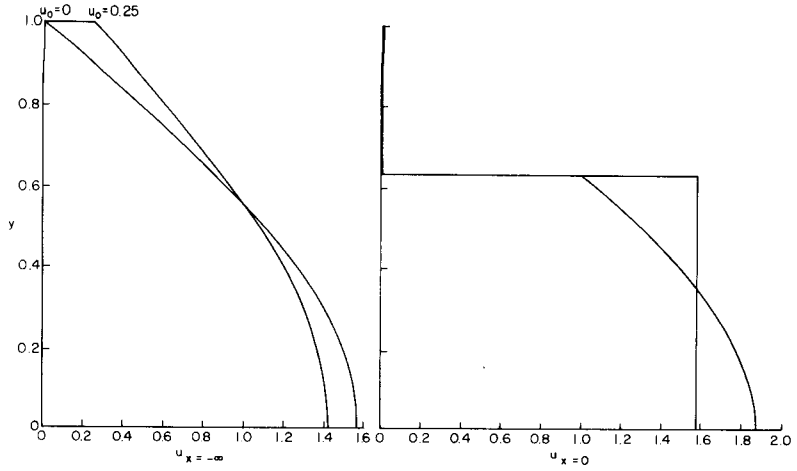

Fig. 4 Typical upstream and exit profiles for channel contractions, $h' = 2/\pi$

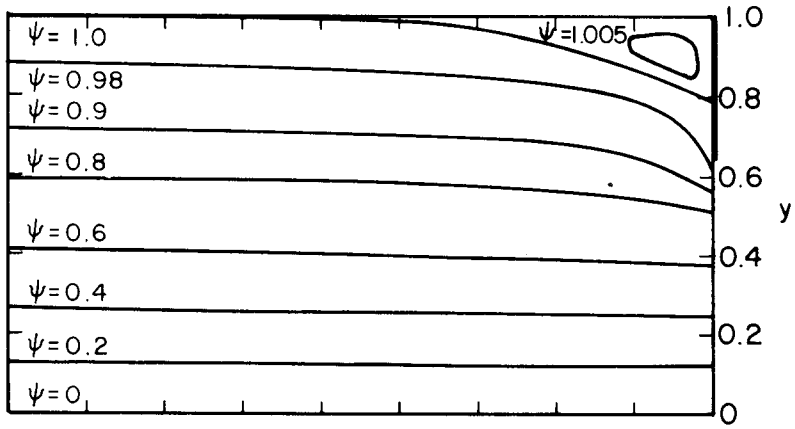

Fig. 5 Channel flow into a contraction, $u_0 = 0.0$, $H = 0.376$, $-u_0 = 2.47$, $h' = 2/\pi$, uniform flow outlet

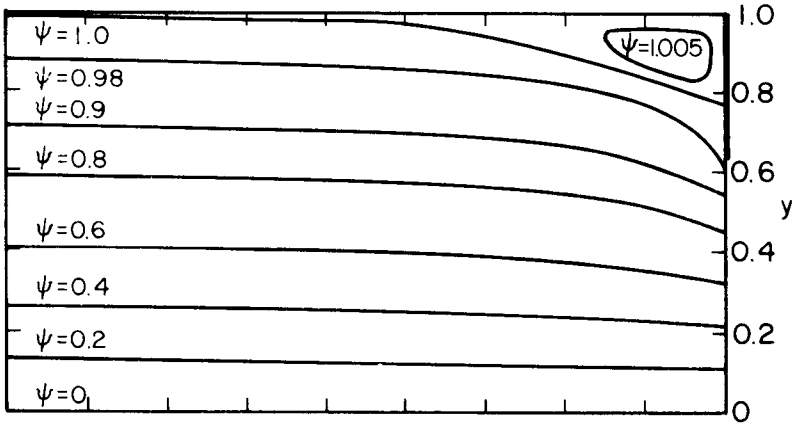

Fig. 6 Channel flow into a contraction, $u = 0.0$, $H = 0.376$, $-u_0 = 2.47$, $h' = 2/\pi$, cosine flow outlet

where

$$C1_n = 2u_0\sin(n\pi h')/(n^2\pi^2 h'), \text{ and} \quad (11)$$

$$C2_n = 2(1-u_0)(\sin(n\pi h')/(n\pi h') + \cos(n\pi)/(4n^2-1))/(n\pi).$$

Similarly the new third boundary condition for the partial cosine velocity profile outlet case is

$$\text{(iii)}\ \psi = \sin(\pi y/2)/\sin(\pi h'/2), \text{ for } -h' < y < h', \text{or} \quad (12)$$
$$= +1 \text{ for } h' \le y \le 1, \text{or}$$
$$= -1 \text{ for } -1 \le y \le -h'.$$

The final solution for stream function is the same as equation (9), but the Fourier coefficients are

$$C1_n = 2u_0/(n\pi)(\cos(n\pi h') - 4n^2\cos(n\pi h')/(4n^2-1) \quad (13)$$
$$+2\sin(n\pi h')\cos(\pi h'/2)/(4n^2-1)/\sin(\pi h'/2), \text{and}$$
$$C2_n = 2(1-u_0)/(n\pi)(\cos(n\pi h') + \cos(n\pi)/(4n^2-1)$$
$$-4n^2\cos(n\pi h')/(4n^2-1)$$
$$+2n\sin(n\pi h')\cos(\pi h'/2)/(4n^2-1)/\sin(\pi h'/2)).$$

Equations (10) and (11) and equations (10) and (13) are the solutions for channel flow into a contraction with uniform

Table 2 Influence of contraction on separation and reattachment

u_0	Outlet Profile	$-\omega_0$	H	h	x_s/h	y_r/h
0	unif.	2.47	0.376	1.000	$-\infty$	0.40
0	unif.	2.47	0.376	0.500	$-\infty$	0.59
0	unif.	2.47	0.376	0.363	$-\infty$	0.58
0	unif.	2.47	0.376	0.200	$-\infty$	0.42
0.10	unif.	2.22	0.417	0.363	−1.21	0.52
0.25	unif.	1.85	0.485	0.363	−1.61	0.39
0.50	unif.	1.24	0.619	0.363	−0.25	0.15
0.75	unif.	0.62	0.784	0.363	~0	~0
1.00	unif.	0.00	1.000	0.363	0.00	0.00
0	cosine	2.47	0.376	1.000	$-\infty$	0.40
0	cosine	2.47	0.376	0.500	$-\infty$	0.61
0	cosine	2.47	0.376	0.363	$-\infty$	0.64
0	cosine	2.47	0.376	0.200	$-\infty$	0.66
0.15	cosine	2.10	0.439	0.500	−1.17	0.52
0.15	cosine	2.10	0.439	0.363	−1.15	0.53
0.15	cosine	2.10	0.439	0.200	−1.06	0.57
0.15	cosine	2.10	0.439	0.100	−0.98	0.51
0.25	cosine	1.85	0.485	1.000	−1.51	0.33
0.25	cosine	1.85	0.485	0.500	−0.74	0.44
0.25	cosine	1.85	0.485	0.363	−0.73	0.46
0.25	cosine	1.85	0.485	0.200	−0.62	0.40

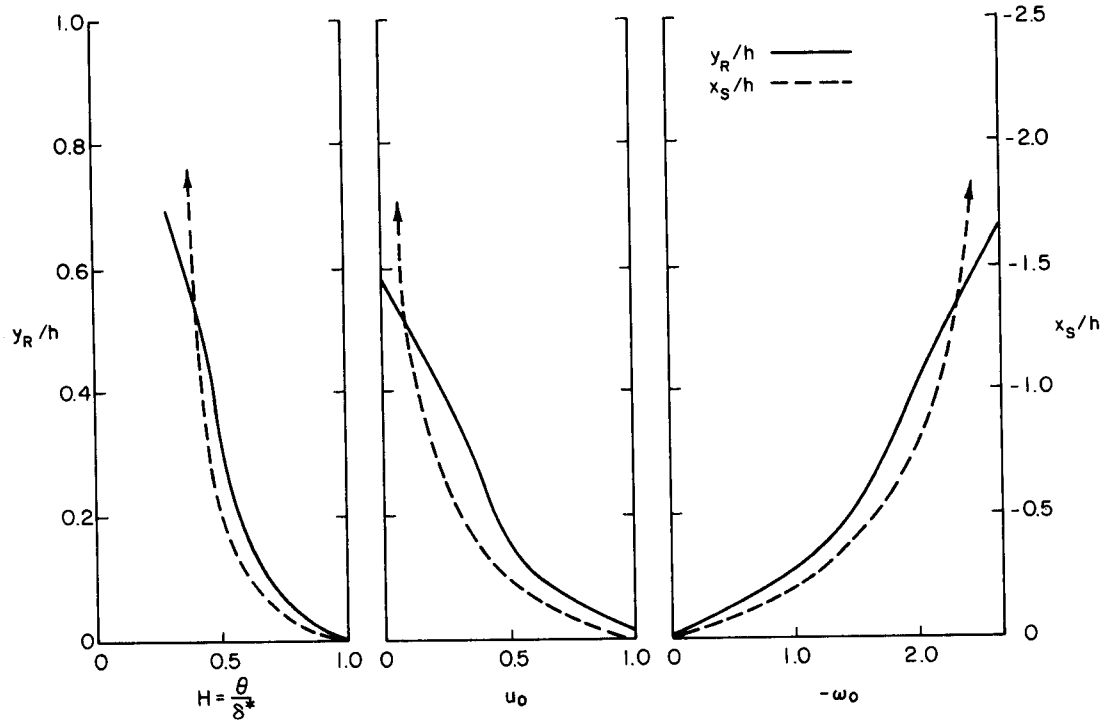

Fig. 7 Variation of separation distance and reattachment distance with profile parameters, $h' = 2/\bar{\pi}$

and partial cosine output profiles respectively. The series solution has been evaluated out to sufficient terms such that the stream function is known to at least five significant places for different values of u_0. Figures 5 and 6 display derived flow patterns for the half channel. As before the stream function is specified to vary between -1 to $+1$ across the channel, but the flow may be distributed in a variety of profiles. Table 2 summarizes cases examined in this paper. Of interest is the relative location of the separation and reattachment points relative to the step height, h.

The size of the corner eddy and its variation with shape factor, slip velocity, and wall vorticity are plotted in Fig. 7 for a fixed size contraction. As slip velocity approaches one, shape factor approaches one, or vorticity decreases the corner eddy disappears. As slip velocity decreases, shape factor decreases, and wall vorticity increases the reattachment point moves toward a value of y_r/h near 0.6, but the separation point moves to $-\infty$.

Alternatively one can examine the variation of eddy size for fixed approach profile as the size of the contraction changes profiles. As the value of h' increases (or h decreases) it requires a larger number of terms from the series to produce a stable result. In general, the corner eddy occupies a larger proportion of the corner as the step increases.

It would be most interesting to compare the results developed here to experimental measurements or other analyses. Unfortunately most previous measurements upstream from a forward facing step are for relatively thin boundary layers developing independently from a constraining opposite wall (Bradshaw and Galea, 1967; Good and Joubert, 1968, Robertson and Taulbee, 1969; Pande et al., 1980). Some authors discuss measurements for large steps in channels but discuss downstream behavior only (Foss, 1962; Emery and Mohsen, 1968).

As noted by most authors, maximum pressures in the corner occur at the reattaching streamline. The separation bubble usually extends about one step height upstream and extends up about 60 percent on the upstream face of the

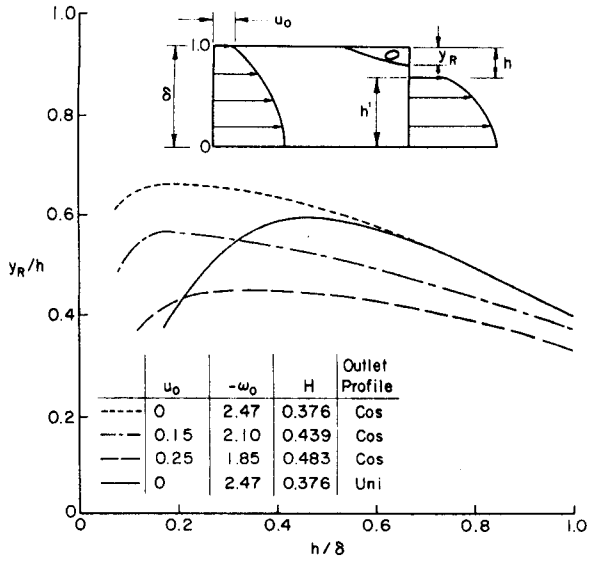

Fig. 8 Variation of reattachment distance with contraction size

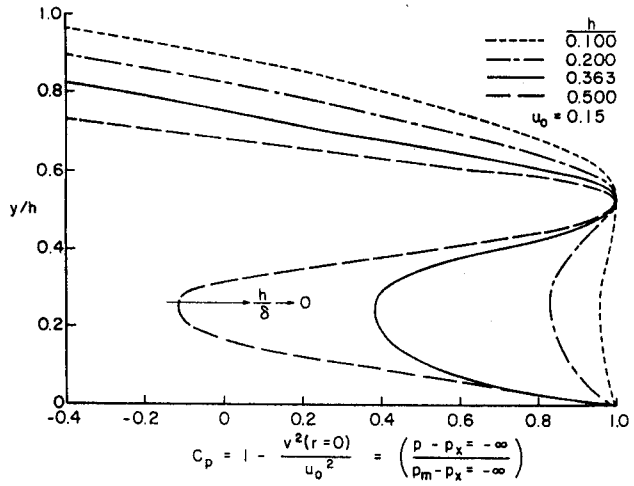

Fig. 9 Pressure distribution on forward facing step wall, $u_0 = 0.15$, $h = 0.1$ to 0.5, cosine flow outlet

contraction. Surface presssures upstream of the contraction on the channel wall begin to increase about 10 step heights upstream of the plate and become maximum on the corner. The pressure distribution displays a double maximum – one at separation, a decrease to reflect corner eddy velocities, and a second maximum on the wall (Bradshaw and Galea, 1967; Good and Joubert, 1968; Taulbee and Robertson, 1972). Sizeable back flow velocities were noted in the corner eddy during the present calculations. Foss (1962) mentioned a similar phenomenon during his channel flow measurements, but for the unconfined step most authors found eddy velocities were one-third or less in magnitude than the main stream velocities. Thus, whereas Taulbee and Robertson (1972) and Good and Joubert (1968) observed only about ten percent variation in the upstream face pressure coefficients over the bottom sixty percent of the corner, the more confined corners exhibited large pressure deviations as the contraction size varied. Good and Joubert (1968) noted that the pressure distribution flattened as the step height decreased, and the same behavior is seen in the exact channel flow contraction calculations (See Figure 9).

Taulbee and Robertson (1972) also observed that for thin boundary layers approaching tall steps choice of the wall vorticity and slip velocity did not seem crucial when predicting experimental measurements by numerical inviscid shear calculations, but that a large near wall vorticity seemed necessary to produce a corner eddy when the boundary layer to step height ratio became large. During the exact calculations considered here the corner eddy generally disappeared as the wall vorticity decreased.

Conclusions

This paper is concerned with deducing features of the corner eddy which forms in two-dimensional channel flow contractions from exact solutions of inviscid shear flow models for the flow motions. Corner eddy shapes are calculated for a line sink and various channel contractions when the upstream flow varied from uniform to a cosine shape. The separation distance from the corner is a direct function of the assumed slip velocity. The reattachment point occurred at 0.4 to 0.6 of the distance from the corner to the edge of the contraction.

References

Bradshaw, P., and Galea, P. V., "Step-Induced Separation of a Turbulent Boundary Layer in Incompressible Flow," *J. Fluid Mechanics*, Vol. 27, Part 1, 1967, pp. 111-130.

Emery, A. F., and Mohsen, A. M., "An Experimental Study of the Separated Flow of Very Thick Incompressible Turbulent Boundary Layers," ASME Paper 68-WA/FE-36, Winter Annual Meeting, December, 1968.

Foss, J. F., "Imcompressible Flow Over a Forward Facing Step," M. S. Thesis, in Mechanical Engineering, Purdue University, June 1962.

Frenkiel, L. E., "On Corner Eddies in Plane Inviscid Shear Flow," *J. Fluid Mechanics*, Vol. 11, Part 3, 1961, pp. 400-406.

Good, M. C., and Joubert, P. N., "The Form Drag of Two-dimensional Bluff Plates Immersed in Turbulent Boundary Layers," *J. Fluid Mechanics*, Vol. 31, Part 3, 1968, pp. 547-582.

Kiya, M., and Arie, M., "A Free-Streamline Theory for Bluff Bodies Attached to a Plane Wall," *J. Fluid Mechanics*, Vol. 56, Part 2, 1972, pp. 201-219.

Bouwmeester, R. J., Meroney, R. N., and Sandborn, V. A., Sites for Wind Power Installations, Wind Flow Over Ridges: Final Report, Dept. of Energy Contract Report No. RLO/243 8-77/1, Colorado State University, Civil Engineering Department CER77-78RJB-RNM-VAS51, 1978, pp. 206.

Miles, J. W., "Upstream Boundary-layer Separation in Stratified Flow," *J. Fluid Mechanics*, Vol. 48, Part 4, 1971, pp. 791-800.

Pande, P. K., Prakash, R., and Agarwal, M. L., "Flow Past Fence in Turbulent Boundary Layers," *J. Hydraulics Division, ASCE*, Vol. 106, No. HY1, 1980, pp. 191-207.

Robertson, J. M., and Taulbee, D. B., "Turbulent Boundary Layer and Separation Flow Ahead of a Step," *Developments in Mechanics*, Vol. 5, (Proceedings of the 11th Midwestern Mechanics Conference), 1969, pp. 171-190.

Taulbee, D. B., and Robertson, J. M., "Turbulent Separation Analysis Ahead of a Step," ASME *Journal of Basic Engineering* Vol. 94, 1972, pp. 544-550.

Thwaites, B., *Incompressible Aerodynamics*, Clarendon Press, Oxford, 1960, pp. 636.

Wu, T. Y., "Cavity and Wake Flows," "*Annual Review of Fluid Mechanics*," Vol. 4, 1972, pp. 243-284.

Yih, C. S., "Two Solutions for Inviscid Rotational Flow with Corner Eddies," *J. Fluid Mechanics*, Vol. 5, 1959, pp. 36-39.